NASA
Technical
Paper
3306

1993

# Ferruleless Coupled-Cavity Traveling-Wave Tube Cold-Test Characteristics Simulated With Micro-SOS

Dana L. Schroeder
*Ohio Aerospace Institute*
*Brook Park, Ohio*

Jeffrey D. Wilson
*Lewis Research Center*
*Cleveland, Ohio*

National Aeronautics and
Space Administration

Office of Management

Scientific and Technical
Information Program

## Summary

The three-dimensional, electromagnetic circuit analysis code, Micro-SOS, can be used to reduce expensive and time-consuming experimental "cold-testing" of traveling-wave tube (TWT) circuits. The frequency-phase dispersion and beam interaction impedance characteristics of a ferruleless coupled-cavity traveling-wave tube slow-wave circuit were simulated using the code. Computer results agree closely with experimental data. Variations in the cavity geometry dimensions of period length and gap-to-period ratio were modeled. These variations can be used in velocity taper designs to reduce the radiofrequency (RF) phase velocity in synchronism with the decelerating electron beam. Such circuit designs can result in enhanced TWT power and efficiency.

## Introduction

Micro-SOS is a three-dimensional, finite-difference, electromagnetic plasma physics simulation code that was developed by Mission Research Corporation (MRC) in cooperation with Varian Associates, Inc. (refs. 1 to 3). Micro-SOS is a version of the MRC code SOS (Self Optimized Sector) but differs in that it does not have the capability to simulate charged particle trajectories. It can be operated in either a time-domain algorithm in which Maxwell's time-dependent equations are solved, or a frequency-domain algorithm (as in this report) in which the resonant mode frequencies and field patterns are obtained.

Micro-SOS was developed by MRC as part of a DOD- and NASA-sponsored effort to develop software for microwave tube design. This code can provide a fast, inexpensive circuit analysis capability that can be used to obtain "cold-test" information about the electromagnetic fields in a microwave tube circuit. The term "cold-test" refers to evaluation of a circuit without the presence of an electron beam. Cold-test measurements are typically performed in the laboratory on actual- or scaled-size circuit models. Using Micro-SOS can potentially eliminate the need for these time-consuming and costly hardware cold-test measurements and greatly facilitate the design of conventional and advanced microwave tube circuits.

In this report, Micro-SOS was used to determine the frequency-phase dispersion and beam interaction impedance characteristics of a single standard cavity of the slow-wave circuit used in the Hughes Aircraft Company Model 951H TWT (traveling-wave tube). This ferruleless coupled-cavity circuit was used in a 29- to 30-GHz, 400-W, low-distortion TWT designed and built by Hughes Aircraft Company under contract to NASA Lewis Research Center (NAS3-24899) (ref. 4). The computer results for both the dispersion and impedance characteristics are compared with experimental data. Variations in the cavity geometry dimensions of period length and gap-to-period ratio were modeled and the effects on dispersion and impedance were simulated. Results from these simulations serve as a basis for designs of circuit modifications that can improve radiofrequency (RF) efficiency or bandwidth.

## Symbols

| | |
|---|---|
| $b$ | electron beam radius |
| $c$ | speed of light |
| $E_{z1}$ | amplitude of first forward-wave space harmonic of axial electric field on the $x_3$-axis |
| $f$ | frequency |
| $h$ | gap length |
| $I_0$ | modified Bessel function of zero$^{th}$ order |
| $I_1$ | modified Bessel function of first order |
| $K_{1,axis}$ | beam interaction impedance of first forward-wave space harmonic on the $x_3$-axis |
| $K_{1,beam}$ | finite beam interaction impedance of first forward-wave space harmonic |
| $L$ | cavity period |
| $L_0$ | standard cavity period |

| | |
|---|---|
| $l$ | gap thickness |
| $N$ | number of cavities |
| $P_{TOT}$ | total RF power flow |
| $R$ | cavity radius |
| $R_0$ | standard cavity radius |
| $r$ | beam tunnel radius |
| $r_-$ | coupling slot inner radius |
| $r_+$ | coupling slot outer radius |
| $t$ | web thickness |
| $v_g$ | group velocity |
| $W_{TOT}$ | total electromagnetic energy stored in cavity |
| $x_1$ | horizontal coordinate |
| $x_2$ | vertical coordinate |
| $x_3$ | axial coordinate |
| $\beta_1$ | axial phase constant of first forward-wave space harmonic |
| $\gamma_1$ | radial phase constant of first forward-wave space harmonic |
| $\theta$ | coupling slot angle |
| $\lambda_1$ | axial wavelength of first forward-wave space harmonic |
| $\omega$ | angular frequency |

## Background

The slow-wave circuit of the Hughes 951H TWT consists of alternating copper webs and spacers (fig. 1) which form a chain of ferruleless cavities. The total circuit of the 951H TWT contains 119 cavities divided into three sections, with a mild double-step velocity taper in the output section (ref. 4).

In order to accurately simulate the electrical characteristics of a TWT with a coupled-cavity computer model (e.g., ref. 5), input is required for both beam interaction impedance and RF phase shift per cavity period. The frequency dependence of the RF phase shift per cavity period is known as the dispersion relationship. In the past, this information was determined experimentally by cold-test measurements of resonant frequencies of a short-circuited length of the circuit (refs. 6 to 8).

As shown herein, Micro-SOS can be used instead of experimental cold-testing to accurately obtain dispersion characteristics and beam interaction impedance for the cavity mode of a ferruleless coupled-cavity TWT slow-wave circuit.

## Simulation

Figure 1 shows the ferruleless coupled-cavity circuit and table I gives the dimensions. A single cavity is modeled on a Cartesian grid divided into 19 ($x_1$-direction) x 33 ($x_2$-direction) x 9 ($x_3$-direction) cells, totaling 5643 cells. Figure 2 shows the $x_1$-$x_2$ cross-sectional grid.

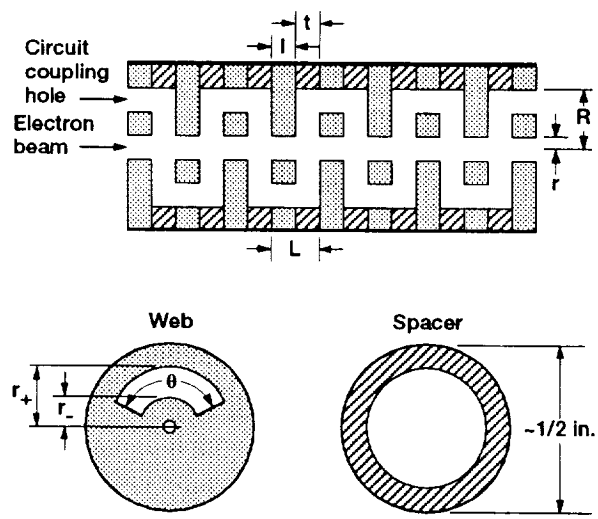


Figure 1.—Ferruleless coupled-cavity TWT circiut.

TABLE I.—DIMENSIONS OF HUGHES 951H 29- TO 30-GHz FERRULELESS COUPLED-CAVITY TWT CIRCUIT
[See fig. 1.]

| Parameter | Dimensions, mm |
|---|---|
| Period, $L$ | 2.0828 |
| Gap thickness, $l$ | 1.0414 |
| Web thickness, $t$ | 1.0414 |
| Cavity radius, $R$ | 2.7559 |
| Beam tunnel radius, $r$ | .5588 |
| Coupling slot inner radius, $r_-$ | 1.2700 |
| Coupling slot center radius, $r_+$ | 2.7432 |
| Coupling slot angle, $\theta$ | 141° |

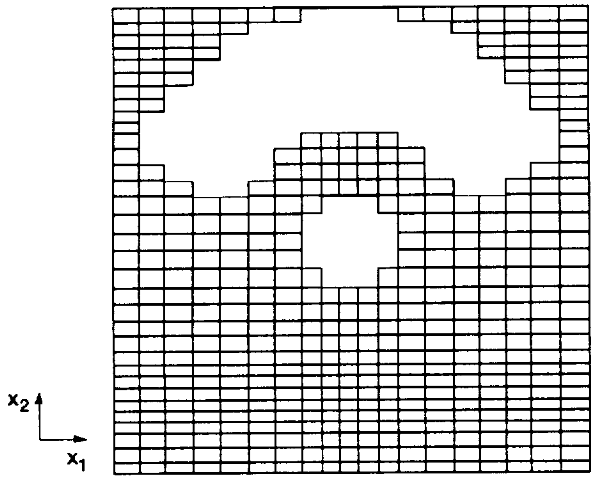


(a) $x_1$-$x_2$ cross section at web.

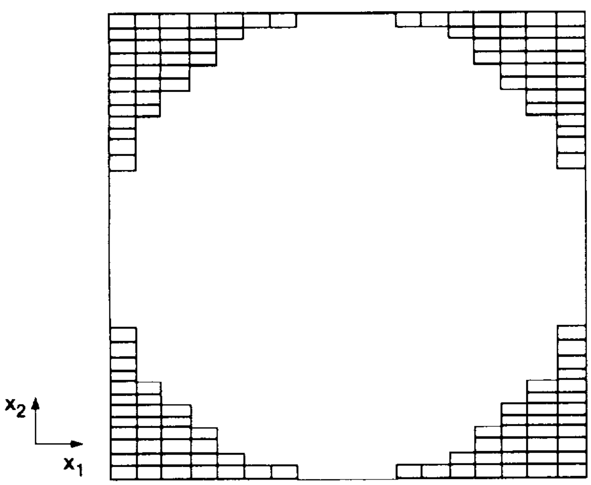


(b) $x_1$-$x_2$ cross section at spacer.

Figure 2.—Micro-SOS grid.

The procedure used for calculating the frequency-phase dispersion characteristics is similar to that used by Kantrowitz and Tammaru (ref. 9) for a coupled-cavity circuit using the computer code ARGUS, a three-dimensional, electrodynamic circuit analysis code developed by Science Applications International Corporation (ref. 10). Kantrowitz and Tammaru obtained a dispersion curve by calculating the three resonant frequencies at the values of RF phase shift per cavity period of $\pi$, $1.5\pi$, and $2\pi$. These resonant frequencies were obtained with three separate computer runs, each with different boundary conditions on a single cavity. Similarly, Doniger et al. (ref. 3) calculated a dispersion curve for a "millitron" coupled-cavity TWT slow-wave circuit by using Micro-SOS. In addition to the single-cavity-calculated resonant frequencies, they used resonant frequencies at $5\pi/4$ and $7\pi/4$, calculated with a single computer run on a two-cavity configuration with appropriate boundary conditions.

This report documents the first time that the frequency-phase dependence of the beam interaction impedance for a coupled-cavity TWT is calculated by using a three-dimensional, electromagnetic circuit analysis code, and compared with experimental results. (Reference 11 reported a similar calculation of impedance for a different slow-wave circuit, but no experimental data was available with which to compare results.)

In the simulations, the cavities were modeled from web center to web center. For all computer runs, each axial boundary was truncated by either an "electric wall" or a "magnetic wall." An electric wall, $E$, is a boundary condition equivalent to a perfectly conducting plane at which the electric field is perpendicular and the magnetic field is parallel. With this boundary condition, the axial electric fields on each side of the boundary are in the same direction (fig. 3). It is simulated with Micro-SOS by using the STRUCTURE CONFORMAL SOLIDIFY command. A magnetic wall, $M$, is a boundary condition that is a symmetry plane with parallel electric fields and perpendicular magnetic fields. With this boundary condition, the axial electric fields on the two sides of the boundary are in opposite directions (fig. 3). It is simulated with Micro-SOS by using the SYMMETRY MIRROR command. Table II summarizes the boundary conditions used to obtain the various resonance points for the dispersion curve of the cavity mode. Table II also shows the run execution times consumed on Lewis' VAX minicomputer (model 9410). As noted, the two-cavity configuration run required considerably more execution time than did the single-cavity configuration runs.

The ferruleless coupled-cavity TWT slow-wave circuit is typically a fundamental backward-wave circuit (ref. 12), with the electron beam interacting primarily with the first forward-wave space harmonic at an RF phase shift per cavity between $\pi$ and $2\pi$ rad (see fig. 4). The beam interaction impedance, known as the Pierce interaction impedance, is a measure of

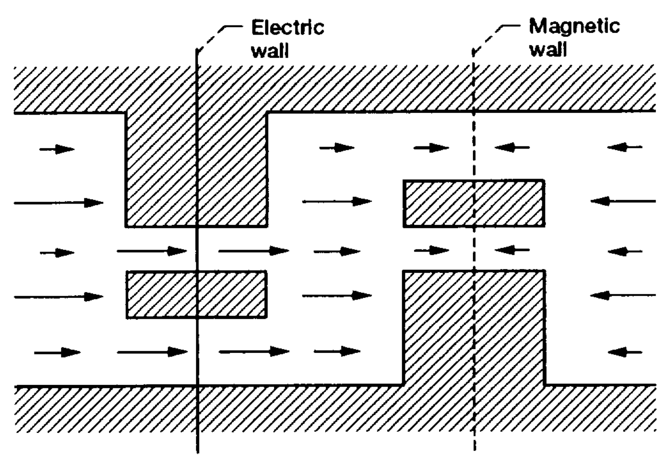


Figure 3.—Axial electric field at electric and magnetic walls. (Radial component of electric field not shown.)

TABLE II.—MICRO-SOS RUNS WITH EXECUTION TIMES CONSUMED ON LEWIS' VAX MINICOMPUTER (MODEL 9410)

| Cavities simulated | Boundary conditions | Phase shift, rad | Execution, time, min:sec |
|---|---|---|---|
| 1 | E,E | $2\pi$ | 0:21 |
| 1 | E,M | $3\pi/2$ | 0:26 |
| 1 | M,M | $\pi$ | 0:28 |
| 2 | E,M | $5\pi/4$, $7\pi/4$ | 1:44 |

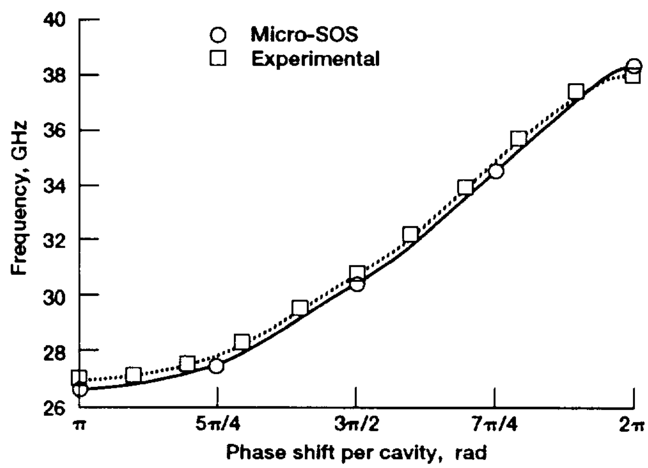


**Figure 4.—Simulated and experimental (ref. 4) phase-frequency dispersion curves for cavity mode.**

the strength of interaction between an RF-wave space harmonic and the electron beam. For the first forward-wave space harmonic, the beam interaction impedance on the axis is given by (ref. 13)

$$K_{1,\mathrm{axis}} = \frac{E_{z1}^2}{2\beta_1^2 P_{TOT}} \tag{1}$$

where $E_{z1}$ is the amplitude of the first forward-wave space harmonic of the axial electric field on the $x_3$-axis, $\beta_1$ is the corresponding axial phase constant, and $P_{TOT}$ is the total RF power flow given by

$$P_{TOT} = \frac{W_{TOT}}{NL} v_g \tag{2}$$

where $N$ is the number of cavities, $L$ is the cavity period, $v_g$ is the group velocity, and $W_{TOT}$ is the total electromagnetic energy stored in the cavity (obtained with Micro-SOS by using the BALANCE and OBSERVE commands). The group velocity for equation (2) is obtained by taking the derivative of the best fitting polynomial curve to the frequency-phase dispersion data and is defined as

$$v_g = \frac{d\omega}{d\beta_1} = 2\omega L \frac{df}{d(\beta_1 L)} \tag{3}$$

To obtain $E_{z1}$ in equation (1), the LINPRINT command is used to print out the axial electric field at the center of each grid cell along the $x_3$-axis at the center of the beam hole. The field is then Fourier analyzed to determine $E_{z1}$.

Note that the beam interaction impedance given in equation (1) is the value on the $x_3$-axis. In simulations with an RF-beam interaction coupled-cavity TWT model (e.g., ref. 5), one must input the impedance integrated over the beam cross-section area. With the assumption that the axial variation of the first forward-wave space harmonic of the electric field is given by $I_0(\gamma_0 r)$ (ref. 14, p. 28), the finite beam interaction impedance is given by

$$K_{1,\mathrm{beam}} = K_{1,\mathrm{axis}} \left[I_0^2(\gamma_1 b) - I_1^2(\gamma_1 b)\right] \tag{4}$$

where $K_{1,\mathrm{axis}}$ is given by equation (1), $b$ is the beam radius, $I_0$ and $I_1$ are modified Bessel functions, and $\gamma_1$ is the radial propagation constant for the first forward-wave space harmonic

$$\lambda_1 = \sqrt{\beta_1^2 - \frac{\omega^2}{c^2}} \tag{5}$$

# Results

## Baseline Circuit

By using the boundary conditions given in table II, resonant frequencies were determined for five values of phase shift for the standard cavity with dimensions given in table I. Table III presents these results, and figure 4 compares the resulting frequency-phase dispersion curve with the experimental curve (ref. 4). The close agreement with the experimental results demonstrates the accuracy of the Micro-SOS simulation. (The Micro-SOS input file used to obtain the resonant frequency at a phase shift of $3\pi/2$ is given in appendix A, and the input file used to obtain the resonant frequencies at phase shifts $5\pi/4$ and $7\pi/4$ is given in appendix B.)

After the dispersion curve was obtained, the group velocity at each value of phase shift was determined from the slope of a best fitting polynomial curve. The resulting group velocities and other parameters needed to calculate the beam interaction impedance from equation (1) are given in table III. Figure 5 plots the calculated impedances; note that agreement with experiment (ref. 4) is excellent. The authors believe that this was the first time that a computer code has been used to accurately simulate the frequency-phase dependence of the beam interaction impedance in a coupled-cavity TWT.

TABLE III.—MICRO-SOS CALCULATIONS COMPARED WITH EXPERIMENT FOR STANDARD CAVITY

| | Phase shift, rad | | | | |
|---|---|---|---|---|---|
| | π (1.00) | 5/4π (1.25) | 3/2π (1.50) | 7/4π (1.75) | 2π (2.00) |
| | Frequency, GHz | | | | |
| Micro-SOS | 26.63 | 27.65 | 30.43 | 34.48 | 38.34 |
| Experiment | 26.80 | 27.82 | 30.70 | 34.86 | 38.24 |
| Difference, % | −.63 | −.61 | −.88 | −1.09 | +.26 |
| | Impedance, Ω | | | | |
| Micro-SOS | ------- | 19.33 | 4.97 | 1.94 | ------- |
| Experiment | ------- | 18.60 | 4.89 | 1.97 | ------- |
| Difference, % | ------- | +3.92 | +1.64 | −1.52 | ------- |

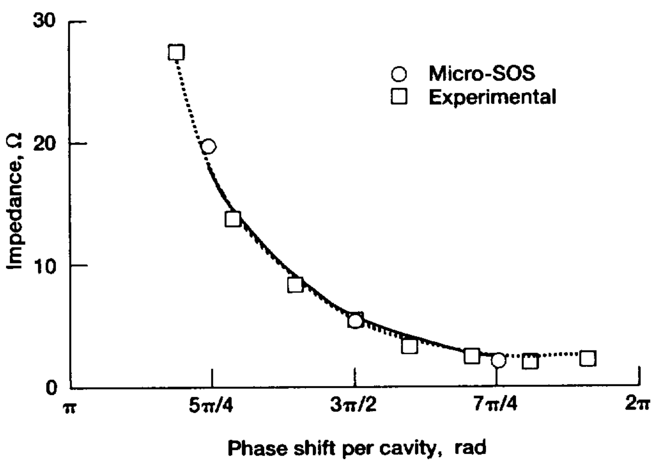


**Figure 5.—Simulated and experimental (ref. 4) beam interaction impedances for cavity mode.**

### Circuit Geometry Variations

The effects on the frequency-phase dispersion curve and interaction impedance of two types of circuit geometry variations were simulated. These variations can be used in velocity taper designs to reduce the RF phase velocity in synchronism with the decelerating electron beam, resulting in enhanced TWT power and efficiency (e.g., ref. 15). Beam interaction impedances were calculated only at a phase shift of 3π/2. Table IV summarizes the frequency-phase dispersion calculations and table V summarizes the beam interaction impedance calculations.

*Cavity Period.*—The first geometry variation simulated was cavity period, the most common geometry variation implemented in a velocity taper design (e.g., ref. 16). As seen in figure 6 and table IV, the frequency decreases with decreasing period when the phase shift is less than 3π/2 and increases with decreasing period when the phase shift is greater than 3π/2. Beam-wave interaction in a coupled-

TABLE IV.—SIMULATED FREQUENCIES (GHz) FOR FREQUENCY-PHASE DISPERSION RELATIONSHIPS
[$L_0$ = 2.0828 mm]

| Case | Variation | Phase shift, rad | | | | |
|---|---|---|---|---|---|---|
| | | π (1.00) | 5/4π (1.25) | 3/2π (1.50) | 7/4π (1.75) | 2π (2.00) |
| 1 | Standard | 26.63 | 27.65 | 30.43 | 34.48 | 38.34 |
| 2 | $L = 0.95L_0$ | 26.51 | 27.57 | 30.44 | 34.60 | 38.38 |
| 3 | $L = .85L_0$ | 26.25 | 27.39 | 30.48 | 34.84 | 38.47 |
| 4 | $L = .75\,L_0$ | 25.98 | 27.21 | 30.51 | 35.07 | 38.57 |
| 5 | $h/L_0 = 0.3$ | 26.17 | 27.09 | 29.60 | 33.00 | 35.24 |
| 6 | $h/L_0 = .4$ | 26.45 | 27.43 | 30.10 | 33.92 | 36.95 |
| 7 | $h/L_0 = .6$ | 26.76 | 27.79 | 30.65 | 34.81 | 39.48 |
| 8 | $h/L_0 = .7$ | 26.84 | 27.89 | 30.79 | 34.99 | 40.44 |

TABLE V.—IMPEDANCE CALCULATIONS AT A PHASE SHIFT OF 3/2π

| Case | Variation | $f$ (GHz) | $v_g$ ($10^7$ m/s) | $\beta_1$ ($m^{-1}$) | $\frac{E_{z1}^2 NL}{2W_{TOT}}$ $\left(10^{15}\frac{kg-m}{A^2s^4}\right)$ | $K_1$ (Ω) |
|---|---|---|---|---|---|---|
| 1 | Standard | 30.43 | 5.96 | 2262 | 1.516 | 4.97 |
| 2 | $L = 0.95L_0$ | 30.44 | 6.16 | 2382 | 1.457 | 4.17 |
| 3 | $L = .85L_0$ | 30.48 | 6.58 | 2662 | 1.250 | 2.68 |
| 4 | $L = .75\,L_0$ | 30.51 | 6.98 | 3017 | 1.093 | 1.72 |
| 5 | $h/L_0 = 0.3$ | 29.60 | 5.31 | 2262 | 1.459 | 5.37 |
| 6 | $h/L_0 = .4$ | 30.10 | 5.75 | ↓ | 1.530 | 5.20 |
| 7 | $h/L_0 = .6$ | 30.65 | 6.03 | | 1.410 | 4.57 |
| 8 | $h/L_0 = .7$ | 30.79 | 6.00 | | 1.200 | 3.91 |

cavity TWT typically takes place at a phase shift close to 5π/4 (ref. 7). At a constant frequency, the phase shift per cavity will increase as the period is decreased, resulting in a decrease in phase velocity.

As the period decreases, the impedance per cavity at a phase shift of 3π/2 decreases rapidly as shown in table V and figure 7. A 25-percent decrease in length from the standard cavity period resulted in a 65-percent decrease in impedance per cavity. This rapid decrease in impedance limits the efficiency that can be obtained in a velocity taper in which the phase velocity is reduced by decreasing the cavity period.

***Gap-to-Period Ratio.***—The second geometry variation simulated was the gap-to-period ratio. This variation could potentially be used in a velocity taper design; however, to the authors' knowledge, it has not been used as such in the past. Table IV and figure 8 show that the frequency decreases with decreasing gap-to-period ratio at all values of phase shift. At a constant frequency, the phase shift per cavity will increase as the gap-to-period ratio is decreased, resulting in a decrease in phase velocity.

As the gap-to-period ratio decreases, the impedance per cavity at a phase shift of 3π/2 increases gradually as shown in

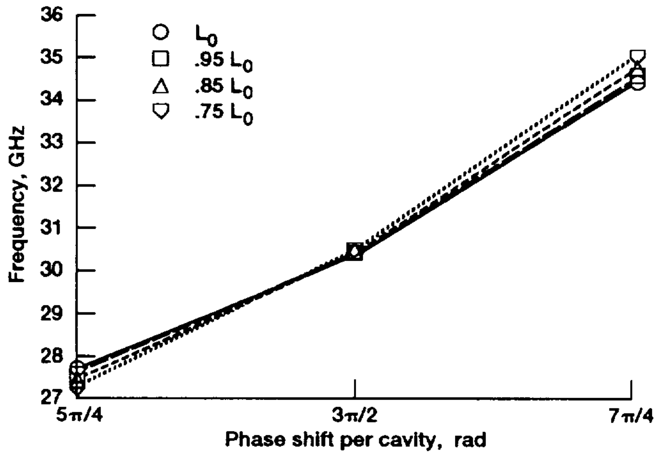


Figure 6.—Simulated phase-frequency dispersion curves for varying cavity periods.

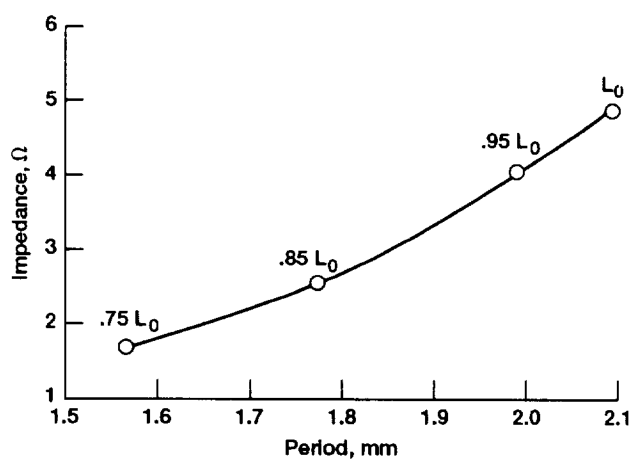


Figure 7.—Simulated beam interaction impedances at a phase shift of 3/2 for varying cavity periods.

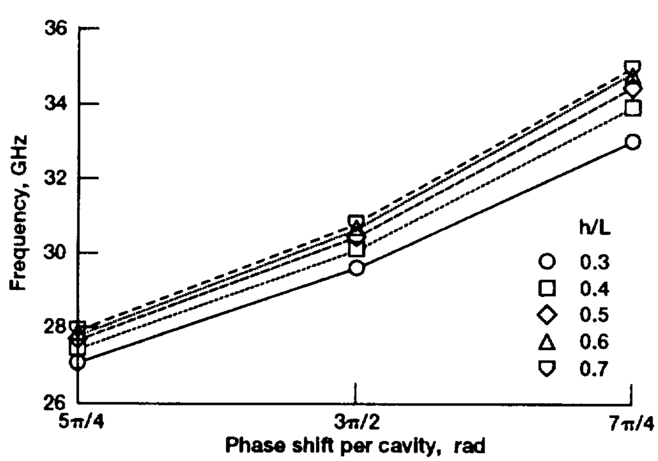


Figure 8.—Simulated phase-frequency dispersion curves for varying gap to period ratios.

table V and figure 9. A 20-percent decrease in gap-to-period ratio from 0.5 to 0.4 resulted in a 4.6-percent increase in impedance. Thus, unlike a velocity taper with a decreasing cavity period, the impedance per cavity could increase in a gap-to-period ratio taper. This suggests that gap-to-period ratio tapers might be able to attain higher efficiencies than those obtained with conventional period taper designs.

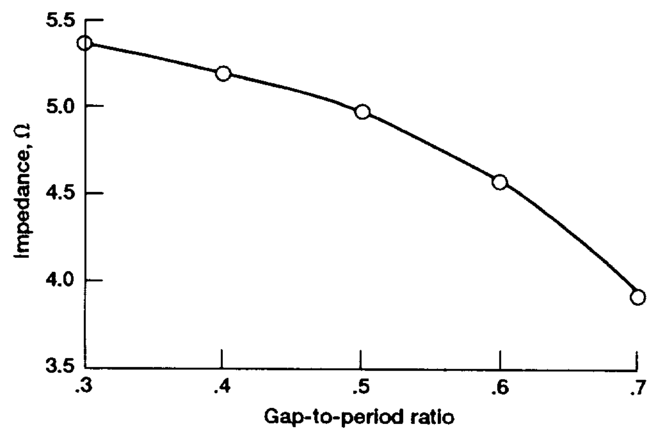


Figure 9.—Simulated beam interaction impedances at a phase shift of 3/2 for varying gap-to-period ratios.

# Conclusions

The usefulness of the electromagnetic circuit analysis computer code Micro-SOS in reducing the need for expensive and time-consuming experimental cold-testing in the design process for traveling-wave tube (TWT) circuits was demonstrated. The code was used to accurately simulate the frequency-phase dispersion characteristics and frequency-phase dependence of the beam interaction impedance for a ferruleless coupled-cavity TWT circuit.

Variations in cavity period and gap-to-period ratio were simulated to determine the effects on frequency-phase dispersion and beam interaction impedance. These variations can be used in velocity taper designs to reduce the RF phase velocity in synchronism with the decelerating electron beam, resulting in enhanced power and efficiency. The simulation results suggest that gap-to-period ratio velocity tapers could enhance power and efficiency more than the conventional cavity-period velocity tapers. Further research is needed to determine the extent of the enhancement and the effect on bandwidth and stability of gap-to-period ratio velocity tapers.

Lewis Research Center
National Aeronautics and Space Administration
Cleveland, Ohio, November 17, 1992

## References


1. Goplen, B.; McDonald, J.; and Warren, G.: SOS Reference Manual, Version October 1988. Mission Research Corporation, Alexandria, VA, Mar. 1989.
2. Goplen, B., et al.: SOS User's Manual, Version October 1988. Mission Research Corporation, Alexandria, VA, Mar. 1989.
3. Doniger, K.J., et al.: Standard Problem Set for Micro-SOS Electromagnetic Circuit Modeling Code, Version October 1988. Varian Associates, Inc., Mar. 1989.
4. Cabrales, M.L., et al.: Study of Methods for the Reduction of Distortion in High Power Traveling-Wave Tubes. NASA CR-185146, 1990.
5. Wilson, J.D.: Revised NASA Axially Symmetric Ring Model for Coupled-Cavity Traveling-Wave Tubes. NASA TP-2675, 1987.
6. Nalos, E.J.: Measurement of Circuit Impedance of Periodically Loaded Structures by Frequency Perturbation. Proc. IRE, vol. 42, no. 10, 1954, pp. 1508–1511.
7. Gittins, J. F.: Power Travelling-Wave Tubes. Elsevier Publishing Co., New York, 1965, pp. 255–265.
8. Horsely, A. W.; and Pearson, A.: Measurement of Dispersion and Interaction Impedance Characteristics of Slow-Wave Structures by Resonance Methods. IEEE Trans. Electron Devices, vol. ED-13, no. 7, 1966, pp. 962–969.
9. Kantrowitz, F.; and Tammaru, I.: Three-Dimensional Simulations of Frequency-Phase Measurements of Arbitrary Coupled-Cavity RF Circuits. IEEE Trans. Electron Devices, vol. 35, no. 11, Nov. 1988, pp. 2018–2026.
10. Mondelli, A., et al.: ARGUS Code Manual User's Guide. Science Applications International Corporation, Apr. 1, 1991.
11. Kory, C.L; and Wilson, J.D.: Simulation of TunneLadder Traveling-Wave Tube Cold-Test Characteristics. Implementation of the Three-Dimensional Electromagnetic Circuit Analysis Code Micro-SOS. NASA TP–3294, 1993.
12. Gilmour, A.S.: Microwave Tubes. Artech House, Inc., Dedham, MA, 1986, pp. 295–303.
13. Gewartowski, J.W.; and Watson, H.A.: Principles of Electron Tubes, Including Grid-Controlled Tubes, Microwave Tubes, and Gaz Tubes. D. Van Nostrand Company, Inc., Princeton, NJ, 1965, p. 357.
14. Pierce, J.R.: Traveling-Wave Tubes. D. Van Nostrand Company, Inc., New York, 1950, p. 28.
15. Wilson, J.D.: Computationally Generated Velocity Taper for Efficiency Enhancement in a Coupled-Cavity Traveling-Wave Tube, IEEE Trans. ED, vol. 36, no. 4, 1989, pp. 811–816.
16. Wilson, J.D., et al.: A High-Efficiency Ferruleless Coupled-Cavity Traveling-Wave Tube with Phase-Adjusted Taper. IEEE Trans. ED, vol. 37, no. 12, 1990, pp. 2638–2643.
17. Connolly, D.J.: Coupled Cavity Traveling Wave Tube with Velocity Tapering. U.S. Patent 4,315,194, Feb. 9, 1982.

# Appendix A

## Micro-SOS Input File for Calculating Resonant Frequencies at Phase Shifts of 3π/2

```
TITLE * FERRULELESS 1 CCTWT * /

COMMENT * DIMENSIONS * /
COMMENT * PERIOD = 2.0828E-03 meters * /
COMMENT * CAVITY RADIUS = 2.756E-03 meters * /
COMMENT * BEAM HOLE RADIUS = 5.588E-04 meters * /
COMMENT * BEAM TUBE RADIUS = 1.27E-03 meters * /
COMMENT * COUPLING SLOT ANGLE = 140.0 degrees * /
COMMENT * GAP = 1.0414E-03 meters * /
COMMENT * WEB(WALL) = 1.0414E-03 meters  HALF = 5.207-04 meters * /
COMMENT * GAP/PERIOD RATIO = 0.5 * /

COMMENT * MAKE GRID * /

COMMENT * NOTE THAT THE CENTER OF X1 IS AT 0.0. * /
COMMENT * THE 5 REPRESENTS THE BEAM HOLE. * /
X1GRID FUNCTION 20 1 -0.002756       7 0.0003138   0.0021970
                                     5 0.0002236   0.0011176
                                     7 0.0003138   0.0021970 /

COMMENT * THE 10's BELOW REPRESENT THE WALL OF THE CAVITIES. * /
COMMENT * THE TWO EQUAL 4's REPRESENT THE BEAM TUBE. * /
COMMENT * THE MIDDLE 5 REPRESENTS THE BEAM HOLE. * /
COMMENT * NOTE THAT THE CENTER OF X2 IS AT 0.0. * /
X2GRID FUNCTION 34 1 -0.002756      10 0.00014859  0.0014859
                                     4 0.0001778   0.0007112
                                     5 0.0002236   0.0011176
                                     4 0.0001778   0.0007112
                                    10 0.00014859  0.0014859 /

COMMENT * THE 2's REPRESENT THE WEB HALVES ON THE SIDES. * /
COMMENT * THE 5 REPRESENTS THE CAVITY GAP. * /
COMMENT * NOTE THAT THE CENTER OF X3 IS AT 0.0. * /
X3GRID FUNCTION 10 1 -0.0010414      2 0.00026035  0.0005207
                                     5 0.00020828  0.0010414
                                     2 0.00026035  0.0005207 /

COMMENT * FORM THE MAIN CAVITY * /

COMMENT * BY FIRST SOLIDIFYING THE ENTIRE VOLUME * /
COMMENT * AND ADDING CONDUCTING BOUNDARIES * /
STRUCTURE CONFORMAL SOLIDIFY      +1   0 21  0 35  0 11 /

COMMENT * THEN VOID OUT THE INSIDE AS A CYLINDER * /
COMMENT * TO FORM THE CIRCULAR CAVITIES. * /
STRUCTURE CYLINDER CAVITY         -1   CARTESIAN  0.0 0.0 -0.0010414
                                       3 0.0  1 0.0  0.002756 0.0020828 /

SYMMETRY MIRROR                   +1   1 20  1 34  1 1 /
C SYMMETRY MIRROR                   -1   1 20  1 34  10 10 /

COMMENT * FORM LEFT SIDE * /

STRUCTURE CONFORMAL WALL        +1  1 20  1 34  1 3 /

COMMENT * THIS STATEMENT MAKES THE COUPLING SLOT IN THE FIRST HALF-WALL * /
COMMENT * LONG, ENDING AT -2.0828E-04 m * /14E-03m) AND IS 8.3312E-04 meters * ^
STRUCTURE ELLIPTICAL WEDGEL       -1  CARTESIAN  0.0 0.0 -0.0010414
                                                 0.0 0.0 -0.0005207
```

```
                                        0 1 0      0.002756 0.002756
                                        0 1 0      0.002756 0.002756
                                        -70.0 70.0  -70.0 70.0    /

COMMENT * THIS STATEMENT SOLIDIFIES THE SPACE BETWEEN THE BEAM HOLE AND * /
COMMENT * THE COUPLING SLOT.  IT IS THE SAME LENGTH AS THE SLOT(1.0414E-3m) * /

STRUCTURE CYLINDER PATCHL          +1  CARTESIAN  0.0 0.0 -0.0010414
                                        3 0.0  1 0.0  0.00127 0.0005207 /

COMMENT * FORM RIGHT SIDE * /

STRUCTURE CONFORMAL WALLR          +1  1 20  1 34  8 10 /

COMMENT * THIS STATEMENT MAKES THE COUPLING SLOT IN THE SECOND HALF-WALL * /
COMMENT * IT ENDS AT THE RIGHT EDGE (1.0414E-03m) AND IS 8.3312E-04 meters * /
COMMENT * LONG, STARTING AT 2.0828E-04 m * /
STRUCTURE ELLIPTICAL WEDGER        -1  CARTESIAN  0.0 0.0 0.0005207
                                                  0.0 0.0 0.0010414
                                        0 1 0      0.002756 0.002756
                                        0 1 0      0.002756 0.002756
                                        110.0 250.0  110.0 250.0     /

STRUCTURE CYLINDER PATCHR          +1  CARTESIAN  0.0 0.0 0.0005207
                                        3 0.0  1 0.0  0.00127 0.0005207/

COMMENT * SHOW BEAM HOLE * /

COMMENT * FIRST A BEAMTUBE IS MADE TO ENCLOSE THE BEAM HOLE. * /
STRUCTURE CYLINDER BEAMTUBE        +1  CARTESIAN  0.0 0.0 -0.0010414
                                        3 0.0  1 0.0  0.00127 0.0020828 /

COMMENT * THE PARTS OF THE BEAMTUBE IN THE CAVITIES MUST BE REMOVED. * /
STRUCTURE CONFORMAL GAP            -1  6 16  11 24  3 8 /

COMMENT * THEN THE BEAM HOLE IS FORMED.  * /
STRUCTURE CYLINDER BEAMPORT        -1  CARTESIAN  0.0 0.0 -0.0010414
                                        3 0.0  1 0.0  0.0005588 0.0020828 /


COMMENT * FREQUENCY * /

FREQUENCY  1 10.0E+10  0.001  50000 /
DIAGNOSE FREQUENCY  1 0 1 /

RANGE  1  1  0.0 0.0  3  10 10  17 17  1 10 /

LINPRINT 1 1 3 1 10 10 17 17 1 10 0 0 1 0 0 0 0 0 0 /

BALANCE  1  1 20  1 34  1 10 /
OBSERVE  1  1  ENERGY  1  0.0 0.0  0.0 0.0  TOTAL     0  1 /


COMMENT * VECTOR PLOTS THAT SHOW THE ELECTRIC FIELD * /

COMMENT * X2-X3 PLANE THRU X1 MIDDLE * /
VECTOR  1  1 1 1  E
        2 3  0.0 0.0  -0.003 0.003  -0.0011 0.0011
        15 15 /

COMMENT * X1-X3 PLANE THRU X2 MIDDLE * /
VECTOR  1  1 1 1  E
        1 3  -0.003 0.003  0.0 0.0  -0.0011 0.0011
        15 15 /

COMMENT * X1-X2 PLANE THRU CAVITY (X3=5) * /
VECTOR  1  1 1 1  E
        1 2  -0.003 0.003  -0.003 0.003  0.0 0.0
        15 15  /
```

```
COMMENT * X1-X2 PLANE THRU WALL (X3=2) * /
VECTOR  1  1 1 2  E
        1 2  -0.003 0.003  -0.003 0.003  -0.00036449 -0.00036449
        15 15 /

COMMENT * THESE COMMANDS ARE USED TO SHOW THE STRUCTURE FROM DIFFERENT * /
COMMENT * VIEWPOINTS * /

COMMENT * X2-X3 PLANE ALONG X1 MIDDLE * /
DISPLAY MODEL  1 10 /

COMMENT * X1-X3 PLANE ALONG X2 MIDDLE * /
DISPLAY MODEL  2 17 /

COMMENT * X1-X2 PLANE IN A WALL * /
DISPLAY MODEL  3 2 /

COMMENT * X1-X2 PLANE IN A CAVITY * /
DISPLAY MODEL  3 5 /

START /
STOP /
```

# Appendix B

## Micro-SOS Input File for Calculating Resonant Frequencies at Phase Shifts 5π/4 and 7π/4

```
TITLE * FERRULELESS TWO-CAVITY CCTWT * /

COMMENT * DIMENSIONS * /
COMMENT * PERIOD = 2.0828E-03 meters * /
COMMENT * CAVITY RADIUS = 2.756-03 meters * /
COMMENT * BEAM HOLE RADIUS = 5.588E-04 meters * /
COMMENT * BEAM TUBE RADIUS = 1.27E-03 meters * /
COMMENT * COUPLING SLOT ANGLE = 140.0 degrees * /
COMMENT * GAP = 1.0414E-03 meters * /
COMMENT * WEB(WALL) = 1.0414E-03 meters * /
COMMENT * GAP/PERIOD RATIO = 0.5 * /

COMMENT * MAKE GRID * /

COMMENT * NOTE THAT THE CENTER OF X1 IS AT 0.0 * /
X1GRID FUNCTION 20 1 -0.002756       7 0.000313800 0.0021972
                                     5 0.000223500 0.0011176
                                     7 0.000313800 0.0021972 /

COMMENT * THE 10's BELOW REPRESENT THE WALL OF THE CAVITIES * /
COMMENT * THE TWO EQUAL 4's REPRESENT THE BEAM TUBE * /
COMMENT * THE MIDDLE 5 REPRESENTS THE BEAM HOLE * /
COMMENT * NOTE THAT THE CENTER OF X2 IS AT 0.0 * /
X2GRID FUNCTION 34 1 -0.002756     10 0.00014859  0.0014859
                                    4 0.00017780  0.0007112
                                    5 0.00023250  0.0011176
                                    4 0.00017780  0.0007112
                                   10 0.00014859  0.0014859 /

COMMENT * THE 2's REPRESENT THE WEB HALVES ON THE SIDES * /
COMMENT * THE 4 REPRESENTS THE CENTER WEB * /
COMMENT * THE 5's REPRESENTS THE CAVITY GAP * /
COMMENT * NOTE THAT THE CENTER OF X3 IS AT 0.0 * /
X3GRID FUNCTION 19 1 -0.0020828     2 0.00026040  0.0005207
                                    5 0.00020830  0.0010414
                                    4 0.00026040  0.0010414
                                    5 0.00020830  0.0010414
                                    2 0.00026040  0.0005207 /

COMMENT * FORM THE MAIN CAVITY * /
COMMENT * BY FIRST SOLIDIFYING THE ENTIRE VOLUME * /
COMMENT * AND ADDING CONDUCTING BOUNDARIES. * /
STRUCTURE CONFORMAL SOLIDIFY      +1   0 21  0 35  0 20 /

COMMENT * THEN VOID OUT THE INSIDE AS A CYLINDER * /
COMMENT * TO FORM THE CIRCULAR CAVITIES. * /
STRUCTURE CYLINDER CAVITY         -1   CARTESIAN  0.0 0.0 -0.0020828
                                       3 0.0  1 0.0  0.002756 0.0041656 /

COMMENT * THE 1.25*PI AND 1.75*PI MODES CAN BE FOUND USING A 2-CAVITY * /
COMMENT * STRUCTURE AND ONE SYMMETRY COMMAND AS BELOW. * /
SYMMETRY MIRROR                   +1   1 20  1 34  1 1  /

COMMENT * FORM INSIDE BODY * /

COMMENT * BECAUSE THE STRUCTURE IS ALREADY HOLLOWED OUT, * /
COMMENT * EACH WALL AND SLOT CAN BE FORMED SEPARATELY. * /

COMMENT * FORM CENTER WALL * /
```

```
COMMENT * THE CENTER WEB IS SOLID ALL THROUGH X1 AND X2 * /
COMMENT * BUT TAKES UP 4 GRID SPACES (GRID INDICES 8,9,10,11,12) ALONG X3. * /
STRUCTURE CONFORMAL WALLCTR        +1  1 20  1 34  8 12 /

COMMENT * THIS STATEMENT MAKES THE COUPLING SLOT ALL ALONG THE STRUCTURE, * /

COMMENT * BUT IT IS ONLY USED IN THE CENTER WALL.  THE PARTS OF THE SLOT ON * /
COMMENT * EITHER SIDE OF THE CENTER WALL ARE ERASED BY OTHER COMMANDS. * /
COMMENT * THE SLOT RADIUS IS 2.756E-03 meters AND HAS AN ANGLE OF 140 DEG * /
COMMENT * THE ANGLE IS CENTERED AROUND THE -X2 AXIS, WHICH IS 180 DEGREES * /
STRUCTURE ELLIPTICAL WEDGECTR      -1  CARTESIAN  0.0 0.0 -0.0020828
                                                  0.0 0.0  0.0020828
                                       0 1 0      0.002756 0.002756
                                       0 1 0      0.002756 0.002756
                                       110.0 250.0  110.0 250.0        /

COMMENT * THIS STATEMENT SOLIDIFIES THE SPACE BETWEEN THE BEAM HOLE AND * /
COMMENT * THE COUPLING SLOT.  IT IS THE SAME LENGTH AS THE SLOT (1.0414E-03m)*/
STRUCTURE CYLINDER PATCHCTR        +1  CARTESIAN  0.0 0.0 -0.0005207
                                       3 0.0  1 0.0  0.00127 0.0010414 /

COMMENT * FORM LEFT SIDE * /

COMMENT * THE FIRST HALF-WEB IS SOLID ALL THROUGH X1 AND X2 * /
COMMENT * BUT ONLY TAKES UP 2 GRID SPACES (GRID INDICES 1,2,3) ALONG X3. * /
STRUCTURE CONFORMAL WALLL          +1  1 20  1 34  1 3 /

COMMENT * THIS STATEMENT MAKES THE COUPLING SLOT IN THE FIRST HALF-WALL * /
COMMENT * IT STARTS AT THE LEFT EDGE(-2.0828E-03 m) AND IS 5.207E-04 meters * /
COMMENT * LONG, MAKING IT END AT -1.5621E-03 m. * /
COMMENT * THE SLOT RADIUS IS 2.756E-03 m AND HAS AN ANGLE OF 140 DEGREES * /
COMMENT * THE ANGLE IS CENTERED AROUND THE +X2 AXIS, WHICH IS 0 DEGREES. * /
STRUCTURE ELLIPTICAL WEDGEL        -1  CARTESIAN  0.0 0.0 -0.0020828
                                                  0.0 0.0 -0.0015621
                                       0 1 0      0.002756 0.002756
                                       0 1 0      0.002756 0.002756
                                       -70.0 70.0  -70.0 70.0          /

COMMENT * THIS STATEMENT SOLIDIFIES THE SPACE BETWEEN THE BEAM HOLE AND * /
COMMENT * THE COUPLING SLOT. IT IS THE SAME LENGTH AS THE SLOT (5.207E-04). * /
STRUCTURE CYLINDER PATCHL          +1  CARTESIAN  0.0 0.0 -0.0020828
                                       3 0.0  1 0.0  0.00127 0.0005207 /

COMMENT * FORM RIGHT SIDE * /

COMMENT * THE SECOND HALF-WEB IS SOLID ALL THROUGH X1 AND X2 * /
COMMENT * BUT ONLY TAKES UP 2 GRID SPACES (GRID INDICES 17,18,19) ALONG X3. * /
STRUCTURE CONFORMAL WALLR          +1  1 20  1 34  17 19 /

COMMENT * THIS STATEMENT MAKES THE COUPLING SLOT IN THE SECOND HALF-WALL * /
COMMENT * IT ENDS AT THE RIGHT EDGE(2.0828E-03 m) AND IS 5.207E-04 meters * /
COMMENT * LONG, MAKING IT START AT 1.5621E-03 m. * /
COMMENT * THE SLOT RADIUS IS 2.756E-03 m AND HAS AN ANGLE OF 140 DEGREES * /
COMMENT * THE ANGLE IS CENTERED AROUND THE +X2 AXIS. * /
STRUCTURE ELLIPTICAL WEDGER        -1  CARTESIAN  0.0 0.0 0.0015621
                                                  0.0 0.0 0.0020828
                                       0 1 0      0.002756 0.002756
                                       0 1 0      0.002756 0.002756
                                       -70.0 70.0  -70.0 70.0          /

COMMENT * THIS STATEMENT SOLIDIFIES THE SPACE BETWEEN THE BEAM HOLE AND * /
COMMENT * THE COUPLING SLOT. IT IS THE SAME LENGTH AS THE SLOT (5.207E-04). * /
STRUCTURE CYLINDER PATCHR          +1  CARTESIAN  0.0 0.0 0.0015621
                                       3 0.0  1 0.0  0.00127 0.0005207 /

COMMENT * SHOW BEAM HOLE * /

COMMENT * FIRST A BEAM TUBE IS MADE TO ENCLOSE THE BEAM HOLE. * /
STRUCTURE CYLINDER BEAMTUBE        +1  CARTESIAN  0.0 0.0 -0.0020828
                                       3 0.0  1 0.0  0.00127 0.0041656 /
```

```
COMMENT * THE PARTS OF THE BEAM TUBE IN THE CAVITIES MUST BE REMOVED. * /
STRUCTURE CONFORMAL GAP             -1  6 16   11 24   3 8 /
STRUCTURE CONFORMAL GAP             -1  6 16   11 24   12 17 /

COMMENT * THEN THE BEAM HOLE IS FORMED. * /
STRUCTURE CYLINDER BEAMPORT         -1   CARTESIAN  0.0 0.0 -0.0020828
                                         3 0.0  1 0.0  0.0005588 0.0041656 /

COMMENT * FREQUENCY * /

COMMENT * THE FIRST RESONANCE FOUND IS THE 1.25 CAVITY MODE. * /
COMMENT * THE SECOND IS THE 1.75 CAVITY MODE. * /
FREQUENCY 2  10.0E+10  .001  50000 /
DIAGNOSE FREQUENCY 1 0 1 /


RANGE  1   1 0.0 0.0  3  11 11  17 17  1 19 /
LINPRINT 1 1 3 1 11 11 17 17 1 19 0 0 1 0 0 0 0 0 0 /


BALANCE  1  1 20  1 34  1 19 /
OBSERVE  1  1
         ENERGY 1  0.0 0.0  0.0 0.0  TOTAL     0  1 /


COMMENT * THESE COMMANDS ARE USED TO SHOW THE STRUCTURE FROM DIFFERENT * /
COMMENT * VIEWPOINTS. * /

COMMENT * X2-X3 PLANE ALONG X1 MIDDLE * /
DISPLAY MODEL  1 11 /

COMMENT * X1-X3 PLANE ALONG X2 MIDDLE * /
DISPLAY MODEL  2 17 /

COMMENT * X1-X2 PLANE IN A WALL * /
DISPLAY MODEL  3 2 /

COMMENT * X1-X2 PLANE IN A CAVITY * /
DISPLAY MODEL  3 6 /

COMMENT * VECTOR PLOTS THAT SHOW THE ELECTRIC FIELD * /

COMMENT * X2-X3 PLANE THRU X1 MIDDLE * /
VECTOR   1  1 1 2  E
         2 3  0.0 0.0  -0.003 0.003  -0.0021 0.0021
         15 15 /

COMMENT * X1-X2 PLANE THRU CAVITY (X3=5) * /
VECTOR   1  1 1 2  E
         1 2  -0.003 0.003  -0.003 0.003  -0.001103884 -0.001103884
         15 15 /

COMMENT * X1-X2 PLANE THRU WALL (X3=10) * /
VECTOR   1  1 1 2  E
         1 2  -0.003 0.003  -0.003 0.003  0.0 0.0
         15 15 /

VECTOR   1  1 1 2  E
         1 3  -0.003 0.003  0.0 0.0  -0.0021 0.0021
         15 15 /

START /
STOP /
```

# REPORT DOCUMENTATION PAGE

Form Approved
OMB No. 0704-0188



**1. AGENCY USE ONLY** (*Leave blank*)

**2. REPORT DATE**
August 1993

**3. REPORT TYPE AND DATES COVERED**
Technical Paper

**4. TITLE AND SUBTITLE**
Ferruleless Coupled-Cavity Traveling-Wave Tube Cold-Test Characteristics Simulated With Micro-SOS

**5. FUNDING NUMBERS**
WU-506-723

**6. AUTHOR(S)**
Dana L. Schroeder and Jeffrey D. Wilson

**7. PERFORMING ORGANIZATION NAME(S) AND ADDRESS(ES)**
National Aeronautics and Space Administration
Lewis Research Center
Cleveland, Ohio 44135-3191

**8. PERFORMING ORGANIZATION REPORT NUMBER**
E-7411

**9. SPONSORING/MONITORING AGENCY NAMES(S) AND ADDRESS(ES)**
National Aeronautics and Space Administration
Washington, D.C. 20546-0001

**10. SPONSORING/MONITORING AGENCY REPORT NUMBER**
NASA TP-3306

**11. SUPPLEMENTARY NOTES**
Dana L. Schroeder, Ohio Aerospace Institute, 22800 Cedar Point Road, Brook Park, Ohio 44142 and Summer Student Intern at NASA Lewis Research Center. Responsible person, Jeffrey D. Wilson, NASA Lewis Research Center, (216) 433-3513.

**12a. DISTRIBUTION/AVAILABILITY STATEMENT**
Unclassified - Unlimited
Subject Category 33

**12b. DISTRIBUTION CODE**

**13. ABSTRACT** ***(Maximum 200 words)***
The three-dimensional, electromagnetic circuit analysis code, Micro-SOS, can be used to reduce expensive and time-consuming experimental "cold-testing" of traveling-wave tube (TWT) circuits. The frequency-phase dispersion and beam interaction impedance characteristics of a ferruleless coupled-cavity traveling-wave tube slow-wave circuit were simulated using the code. Computer results agree closely with experimental data. Variations in the cavity geometry dimensions of period length and gap-to-period ratio were modeled. These variations can be used in velocity taper designs to reduce the radiofrequency (RF) phase velocity in synchronism with the decelerating electron beam. Such circuit designs can result in enhanced TWT power and efficiency.

**14. SUBJECT TERMS**
Coupled-cavity; Traveling-wave tube

**15. NUMBER OF PAGES**
16

**16. PRICE CODE**
A03

| 17. SECURITY CLASSIFICATION OF REPORT | 18. SECURITY CLASSIFICATION OF THIS PAGE | 19. SECURITY CLASSIFICATION OF ABSTRACT | 20. LIMITATION OF ABSTRACT |
|---|---|---|---|
| Unclassified | Unclassified | Unclassified | |

NSN 7540-01-280-5500

Standard Form 298 (Rev. 2-89)
Prescribed by ANSI Std. Z39-18
298-102